Photodegradation of a Ternary Iron(III)−Uranium(VI)−Citric Acid Complex

CLEVELAND J. DODGE* AND AROKIASAMY J. FRANCIS

Environmental Sciences Department, Brookhaven National Laboratory, Upton, New York 11973

The mechanisms of photodegradation of binary iron− and uranium−citrate and ternary iron−uranium−citrate complexes were elucidated. Citric acid degradation products were identified by HPLC and GC, and the metal precipitates were identified by XRD and EXAFS. Photodegradation of a binuclear iron−citrate complex occurred as a result of two one-electron oxidations of citric acid with the formation of 3-oxoglutarate and two ferrous ions. The ferrous ions were reoxidized by a photo-Fenton reaction, resulting in the precipitation of iron as two-line ferrihydrite $Fe(OH)_3$. The citric acid in the uranium−citrate complex underwent a two-electron oxidation to acetoacetate with the concomitant reduction of U(VI) to U(IV). The U(IV) was subsequently photooxidized in the presence of dioxygen with precipitation of uranium as the mineral schoepite ($UO_3{\cdot}2H_2O$). A two-step electron reduction of two ferric ions to two ferrous ions was the primary mechanism for photodegradation of the ternary iron−uranium−citrate complex with oxidation of citric acid to 3-oxoglutarate; reduction of uranium was not observed. The iron precipitated as ferrihydrite and the uranyl ion as a uranyl hydroxide species. These results show the potential application of photochemical treatment of wastewater and decontamination solutions containing binary and ternary iron− and uranium−citrate complexes.

Introduction

Citric acid, a naturally occurring hydroxycarboxylic acid, forms different types of complexes with metals, including bidentate, tridentate, binuclear, and polymeric forms. The type of complex formed is dependent upon the pH, oxidation state of the metal, and ratio of metal to citric acid (*1*, *2*). In particular, iron and uranium complexes form binuclear species with citric acid at pH 3.5 and 6.0 (*3*−*7*). However, in the presence of iron and uranium, a ternary iron−uranium−citric acid complex is formed (*5*, *8*, *9*).

Mechanistic studies on the photodecomposition of iron(III)−carboxylate complexes indicate that reduction to Fe(II) is accompanied by oxidative decarboxylation of the carboxylate ligand. The reaction efficiency is dependent on the pH as well as the initial metal-to-ligand ratio (*10*). Exposure of iron−citrate to a mercury vapor lamp resulted in the production of 3-oxoglutaric acid and acetone (*3*). Frahn (*11*) observed that exposure of an equimolar solution of iron and citric acid to sunlight resulted in the reduction of ferric to ferrous ion with the production of 3-oxoglutaric acid and acetoacetate, but the fate of Fe was not determined in these studies.

Exposure of a binary 1:1 uranium−citric acid complex at pH 3.5 to a tungsten lamp produced acetone and carbon dioxide as final products (*12*). Dodge and Francis (*6*) identified acetoacetate as the intermediate product in the photodecomposition of uranium−citrate at pH 3.5. Acetoacetate was further degraded to acetate and acetone. Uranium was reduced to U^{4+} by a two-electron-transfer process with the formation of U^{4+}, which was readily reoxidized in the presence of dioxygen. The uranium precipitated from solution as uranium trioxide ($UO_3{\cdot}2H_2O$).

The photochemical reaction mechanisms for ternary mixed-metal organic systems have not been extensively studied. Natarajan and Endicott (*13*) investigated the tris(bipyridyl)ruthenium(II) photosensitized redox decomposition of cobalt(III)−($[NH_3]_5Br^{2+}$, $-EDTA^-$, $-HEDTA^{2-}$) complexes using flash photolysis. The products were identified as Co(II), $Ru(bipy)_3^{2+}$, and CO_2, which were found in equimolar amounts. Hug et al. (*14*) studied the interaction of Cr(VI) with iron(III)−citrate. The Cr was reduced to Cr(III) and remained in solution in complex form with an unidentified oxidation product of citric acid.

Citric acid is an effective metal chelator for the decontamination of uranium-contaminated soils, steel surfaces, and iron-containing wastes; therefore, the potential for formation of an iron−uranium−citric acid mixed-metal complex exists (*8*, *15*, *16*). Photochemical treatment of these solutions is an attractive option because it has been shown that uranium−citrate and iron−uranium−citrate complexes are recalcitrant to biodegradation (*1*, *6*, *8*). Furthermore, photodegradation of the iron−uranium−citrate complex is of fundamental interest because of the presence of two redox-active metals complexed to citric acid. In this study, we report the photodegradation of a ternary iron−uranium−citric acid complex with a comparison to the binary iron− and uranium−citrate complexes.

Materials and Methods

Preparation of Iron−, Uranium−, and Iron−Uranium−Citric Acid Complexes. Citric acid (100 mM, anhydrous; Sigma, St. Louis, MO) was prepared and standardized by potentiometric titration. Stock solutions (100 mM) of ferric nitrate [$Fe(NO_3)_3{\cdot}9H_2O$] (Mallinckrodt, Paris, KY) and uranyl nitrate [$UO_2(NO_3)_2{\cdot}6H_2O$] (BDH Chemicals; Analar, Poole, U.K.) were prepared and analyzed by inductively coupled plasma-optical emission spectroscopy (ICP−OES).

The binary complexes of 1:1 iron−citric acid and 1:1 uranium−citric acid were prepared to 5 mM, as described elsewhere (*6*, *17*). The mixed-metal 1:1:2 iron−uranium−citric acid complex was prepared by combining equimolar amounts of ferric nitrate and uranyl nitrate to citric acid at pH 3.5 to obtain a molar ratio of 1:1:2 iron−uranium−citric acid and 5 mM final concentration (*8*). The ionic strength was adjusted to 0.1 M with KCl, and the pH was readjusted to 3.5 after overnight equilibration. The complexes were exposed to minimal light during preparation.

Ferrihydrite [$Fe(OH)_3$]. Ferrihydrite was prepared by addition of a fixed amount of 1 M KOH to a solution of ferric nitrate (*18*). The pH of the resulting suspension was adjusted to 7.5, and the precipitate was washed three times with 0.1 M NaCl, recovered by centrifugation, dried overnight at 60 °C, and ground to a fine powder in an agate mortar. The

* Corresponding author phone: (631) 344-7234; fax: (631) 344-7303; e-mail: dodge1@bnl.gov.

10.1021/es011125m CCC: $22.00 © xxxx American Chemical Society
Published on Web 00/00/0000

oxide was analyzed by X-ray powder diffraction and it was identified as two-line ferrihydrite (*19*).

Uranium Hydroxide [$UO_2(OH)_2$]. Uranyl hydroxide was prepared by dissolving uranyl nitrate in deionized water and adjusting the pH to 7.0 with NaOH. The precipitate was collected by centrifugation and washed three times with deionized water, dried overnight at 60 °C, and ground to a fine powder.

Photochemical Degradation. One-hundred milliliters of equimolar iron−citrate, uranium−citrate, or iron−uranium−citrate complex (5 mM) was dispensed into 4 × 250 mL Erlenmeyer flasks fitted with cotton plugs. Triplicate samples of each were placed in a growth chamber fitted with seven 60-W high-output growth lamps and maintained at 26 ± 1 °C. The lamps displayed a broad spectral curve in the visible region from approximately 400 to 700 nm. The light intensity was calibrated with a Biosphere Instruments QSL-100 analyzer, and the total intensity at the sample was 0.18 $m \cdot einstein \cdot m^{-2} \cdot s^{-1}$. The fourth sample flask was placed in the dark as a control.

Chemical Analysis. At selected intervals, an aliquot from duplicate samples was withdrawn and analyzed for changes in the UV−vis absorption spectrum of the metal−citrate complexes, changes in pH, the total metal content of the solution, and the oxidation states of Fe and U. The sample was filtered through a 0.22 μm Millex filter, an aliquot was dispensed into a 1-cm quartz cell, and the absorption spectra for the metal complexes were obtained from 350 to 750 nm using a Hewlett-Packard 8452A diode array scanning UV−vis spectrophotometer. The oxidation states of iron (+2, +3) and uranyl ion in the filtered aliquot were determined spectrophotometrically using *o*-phenanthroline (*20*) and bromo-PADAP methods (*21*), respectively. One sample from each set was left undisturbed so that, at the end of the experiment, sufficient solids could be collected for characterization. The presence of pentavalent uranium species in the sample was monitored at approximately 1500 cm^{-1} (6.9 μm) using a Perkin-Elmer model 283 infrared spectrometer (*22*).

Photodegradation Products of Citric Acid. Citric acid and its photodegradation products were determined by high-pressure liquid chromatography (HPLC) using an Aminex HPX-87H column (Bio-Rad Laboratories, Richmond, CA) with a 0.004 M H_2SO_4 mobile phase. Organic acids were determined by UV−vis detection at 210 nm and the alcohols and carbonyl compounds by refractive index detection (Shimadzu). To confirm the identity of the photodegradation products, an aliquot of the filtered sample was acidified, extracted with chloroform, derivitized as methyl esters using methanol−sulfuric acid−chloroform mix, and analyzed by a Perkin-Elmer Sigma 115 gas chromatograph/mass spectrometer (*6*). A Chrompack WCOT fused-silica capillary column coated with CP-Sil 5CB was used to separate the compounds. Helium was used as a carrier gas, and the column temperature was increased from 50 to 250 °C at 5 °C/min.

Gas Production. Gaseous products formed during photodegradation of the metal−citrate complex were determined on a separate sample. Seventy-five milliliters of the metal−citrate complex solution was placed in a 125 mL serum bottle, capped with a butyl rubber stopper, and placed in the growth chamber. At the end of the exposure, the sample was acidified with perchloric acid, and the headspace gases were analyzed by gas chromatography using a stainless steel column (6.1 m × 3.2 mm) packed with Silica Gel (60/80; Alltech Assoc. no. 5651) and connected to a thermal conductivity detector.

Characterization of Precipitates. The precipitate formed from photodegradation of the metal−citrate complex was recovered by centrifugation, washed three times with 0.1 M $MgCl_2$ and then once with deionized water, and dried overnight at 60 °C. The precipitate was ground to a fine powder in an agate mortar and weighed. Total Fe and U in the sample was determined by ICP−OES following dissolution in 1 M hydrochloric acid (Ultrex).

X-ray Diffraction (XRD). The mineralogical analysis of the precipitates was performed using a Philips model XRG 3100 powder X-ray diffractometer (XRD) with a 40 kV Cu Kα X-ray source and a current of 30 mA. Scans were collected every 0.02° at a rate of 2 s/step. Ferrihydrite and uranyl hydroxide standards and precipitate samples from the photodegradation of iron−citrate, uranium−citrate, and iron−uranium−citrate complexes were placed in an aluminum holder and covered with Kapton tape. The lattice spacing values were compared with information from the literature and the JCPDS-International Centre for Diffraction Data.

Extended X-ray Absorption Fine Structure (EXAFS). Five milligrams of the precipitate was thoroughly mixed with boron nitride (20% w/v), placed in a heat sealed polypropylene bag (0.2 mil), and analyzed on beamline X-11A at the NSLS. Fourier transformed EXAFS spectra were obtained in the fluorescence mode at the uranium L_{III} edge (17.166 keV) using a Lytle detector and an Ar gas-filled ionization chamber. The beam size was 1.0 mmV × 10 mmH. Multiple scans (4−6) were collected for each sample and were averaged to minimize the signal-to-noise ratio. A multistep data analysis process which included background subtraction and normalization of the data to the edge jump height was performed to obtain the raw k^3X-weighted spectra. Fourier transformation of the data resulted in a pseudo-radial distribution function (PRDF) which represents the coordination shells of the near-neighbor atoms surrounding the metal (*23*). Distances were not corrected for actual peak positions and are displaced toward shorter distances because of atom pair phase shifts ($\Delta R \approx 0.3-0.5$ Å) which differ for each neighboring atom. The theoretical EXAFS modeling code FEFF 7.02 was used to calculate the backscattering phase and amplitude information for individual neighboring atoms (*24*). Fitting parameters for the samples then were obtained by comparison with the uranyl hydroxide.

Results

Spectrophotometric Analysis. *1:1 Iron−Citric Acid*. The change in the UV−vis absorption spectrum during the photodegradation of the iron−citrate complex is presented in Figure 1A. The solution was initially a clear reddish brown and exhibited a broad spectrum. A shoulder peak was noted at 453 nm. At 3 h, an increase in intensity of the absorption band was observed because of iron hydrolysis resulting from an increase in pH to 6.43 ± 0.03. At 7 h, the spectrum became broad and featureless and continued to increase in intensity up to 96 h. At 196 h, there was a sharp decrease in the absorption spectrum to below that of the initial complex, at which point all of the Fe was precipitated.

1:1 Uranium−Citric Acid. The change in the UV−vis absorption spectrum during the photodegradation of the uranium−citrate complex is presented in Figure 1B. The solution containing the complex was initially fluorescent yellow and showed fine structure between 400 and 500 nm, typical for the uranium−citrate complex (*6*). At 3 and 7 h, there was an increase in absorption at 555 and 665 nm. The appearance of these peaks is confirmatory for the uranous ion (U^{4+}) (*25*). With additional exposure, there was a loss of uranyl ion fine structure, and a spectrum indicating the presence of a reduced uranium species was not observed. The intensity of the absorption spectrum continued to decrease with exposure to light, and at 196 h, only a slight absorbance was noted. Infrared analysis at 1500 nm (6.9 μm) did not detect pentavalent uranium (U^{5+}), indicating that it most likely was an unstable intermediate.

1:1:2 Iron−Uranium−Citric Acid. The change in the UV−vis absorption spectrum during the photodegradation of the

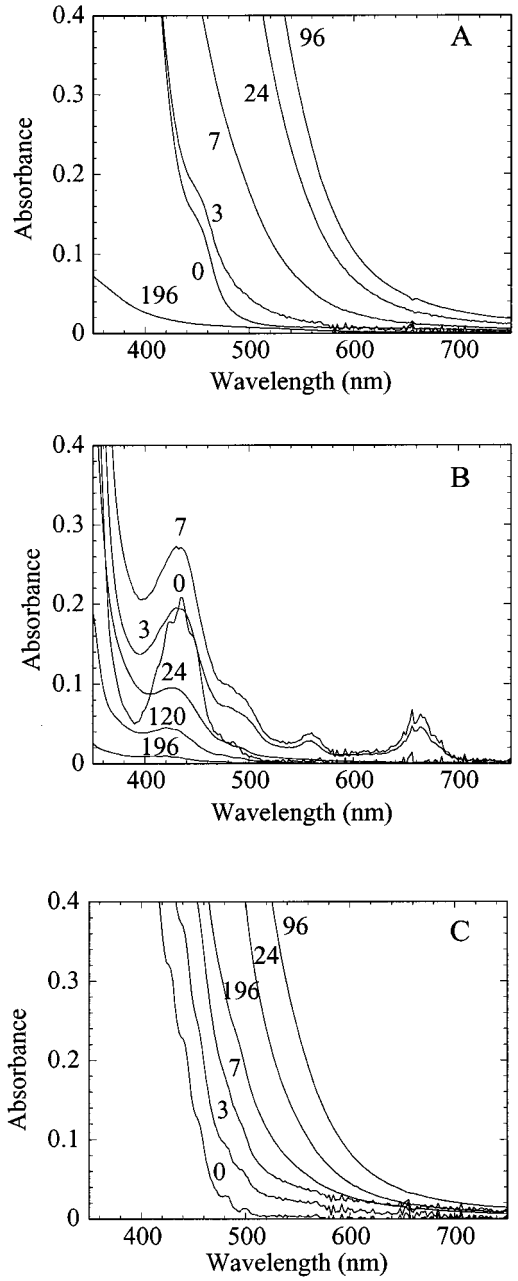

FIGURE 1. Change in UV–vis absorption spectra with irradiation time (h) for 5.0 mM metal–citrate complexes at pH 3.5: (A) 1:1 iron–citric acid, (B) 1:1 uranium–citric acid, and (C) 1:1:2 iron–uranium–citric acid complex.

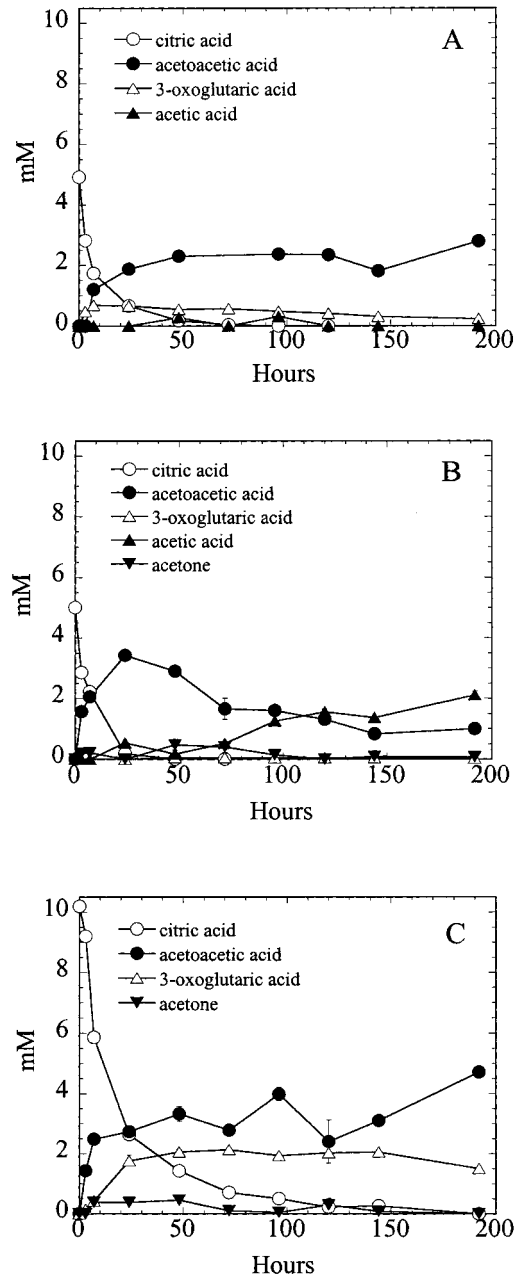

FIGURE 2. Organic metabolite production during photodegradation of (A) 1:1 iron–citric acid, (B) 1:1 uranium–citric acid, and (C) 1:1:2 iron–uranium–citric acid complexes.

iron–uranium–citrate complex is presented in Figure 1C. The initial absorption spectrum is dominated by the presence of ferric ion with three shoulder peaks observed at 427, 440, and 456 nm due to presence of complexed uranyl ion. The absorbance spectrum was less than the sum of the absorbances of the binary complexes, confirming the interaction of Fe and U with citric acid and the formation of a mixed-metal complex (*8*). With increased exposure to light, the spectrum broadened and became featureless between 7 and 96 h. At 196 h, the spectrum absorbance decreased but did not approach baseline values as with the binary complexes. No reduced form of uranium was detected during photodegradation.

Photodegradation Products of Citric Acid. The organic products formed during the photodegradation of the metal–citrate complexes are presented in parts A–C of Figure 2.

1:1 Iron–Citric Acid. The iron–citrate complex was rapidly degraded with citric acid, decreasing to 1.73 ± 0.02 mM (65%) from 4.92 ± 0.10 at a rate of 0.46 mM·h^{-1} in the first 7 h of exposure to light (Figure 2A). The pH increased to 6.44 ± 0.02 from 3.48 ± 0.01. At 72 h, citric acid was completely degraded. The initial photodegradation product formed was 3-oxoglutarate (0.24 ± 0.01 mM). With increased exposure, acetoacetate was formed and reached a maximum of 2.80 ± 0.00 mM at 196 h. Acetate was a minor degradation product which reached a maximum at 96 h (0.31 ± 0.07 mM). The final pH was 7.26 ± 0.20.

1:1 Uranium–Citric Acid. Exposure of the uranium–citrate complex to light resulted in degradation of citric acid to 2.23 ± 0.10 mM (55%) from 5.01 ± 0.13 mM at a rate of 0.40 mM·h^{-1} during the first 7 h (Figure 2B). The pH increased to 4.90 ± 0.00 from 3.48 ± 0.01. The degradation of citric acid was concomitant with the production of acetoacetate, which reached a maximum of 3.43 ± 0.00 mM at 24 h. After that

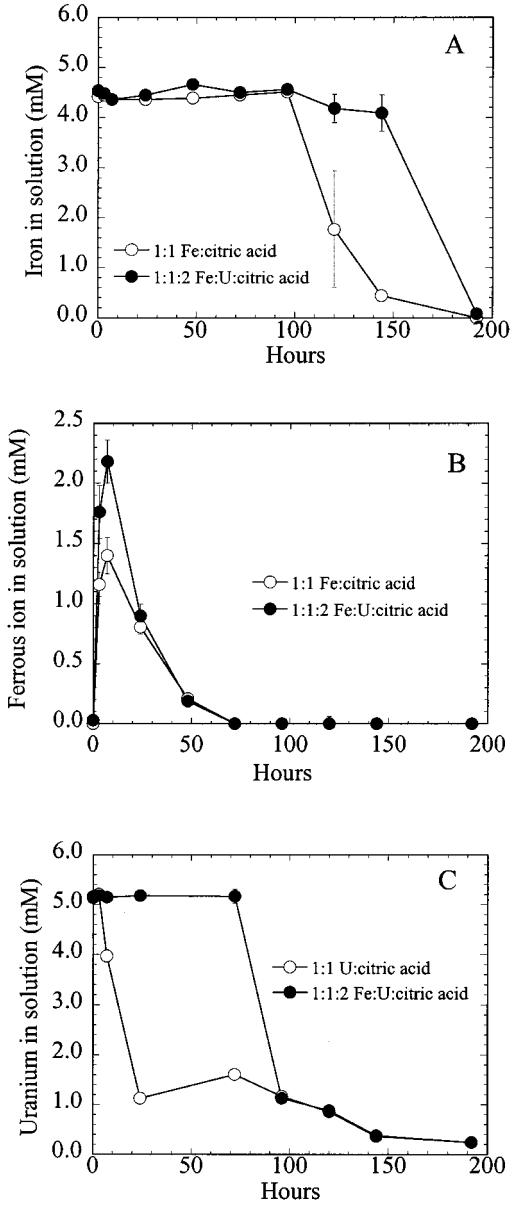

FIGURE 3. Effect of photodegradation on metal remaining in solution following 0.22 μm filtration: (A) total iron, (B) ferrous ion, and (C) uranium.

time, it decreased to 1.00 ± 0.09 mM at 192 h. At 48 h, all of the citric acid was degraded. Acetate gradually increased during the exposure, reaching a maximum of 2.11 ± 0.13 mM at the end of the experiment. Minor amounts of 3-oxoglutarate and acetone were also produced and reached maximum concentrations of 0.05 ± 0.00 mM and 0.47 ± 0.19 mM at 48 h, respectively. The final pH was 5.14 ± 0.01.

1:1:2 Iron–Uranium–Citric Acid. During the first 7 h of exposure to light, citric acid concentration rapidly decreased to 5.87 ± 0.05 (42%) from 10.2 ± 0.10 mM in 7 h at a rate of 0.62 mM·h^{-1} (Figure 2C). The pH increased to 6.34 ± 0.01 from 3.50 ± 0.01. Degradation of citric acid continued at a slower rate thereafter and was completely degraded at 192 h. The concentration of acetoacetate initially increased to 2.49 ± 0.10 mM and reached a maximum of 4.72 ± 0.17 mM at 192 h. The production of 3-oxoglutarate was also significant in the first 24 h of exposure, where it reached a maximum of 2.14 ± 0.07 mM at 72 h and remained constant thereafter. A small amount of acetone was produced and the final pH was 6.96 ± 0.05.

TABLE 1. Iron and Uranium Content of Precipitates from Photodegradation of Metal–Citrate Complexes

complex	precipitate (mg)	iron (% by wt)	uranium (% by wt)
1:1 iron–citric acid	44.2	52.5	
1:1 uranium–citric acid	129		86.7
1:1:2 iron–uranium–citric acid	152	11.2	69.4

Fate of Iron and Uranium During Photodegradation. Figure 3A shows the effect of photodegradation of iron–citrate and iron–uranium–citrate complex on the solubility of iron. Initially, 5.00 ± 0.20 mM iron was present in solution for the iron–citrate complex. After 96 h, the iron concentration decreased only slightly to 4.75 ± 0.20 mM and then rapidly precipitated from solution at 120 h with complete removal at 192 h. In the presence of the iron–uranium–citrate complex, 5.00 ± 0.10 mM iron was present initially. At 144 h, iron decreased slightly to 4.09 ± 0.36 mM, and thereafter, it was rapidly removed (98%) from solution.

Ferrous Ion. Figure 3B shows the production of ferrous ion during photodegradation of iron–citrate and iron–uranium–citrate complexes. In the presence of iron–citrate, ferrous iron was rapidly produced and reached a maximum of 1.40 ± 0.10 mM at 7 h. This coincided with the initial rapid photodegradation of citric acid. Thereafter, it decreased to below the detection limit at 72 h. The production of ferrous iron in the presence of a mixed-metal iron–uranium–citrate complex followed a similar pattern. However, it was produced at a rate and extent greater than the iron–citrate complex, with 2.18 ± 0.18 mM ferrous ion detected at 7 h. The concentration rapidly decreased to below the detection limit at 72 h.

Uranium. Figure 3C shows the effect of photodegradation of uranium–citrate and iron–uranium–citrate complexes on the solubility of uranium. Photodegradation of the uranium–citrate complex resulted in the rapid removal of uranium from solution. At 24 h, uranium concentration decreased to 1.13 ± 0.02 mM (78%) from an initial value of 5.06 ± 0.03 mM. Uranium in solution slowly decreased thereafter to 0.24 ± 0.01 (95%) at 192 h. In the presence of the iron–uranium–citrate complex, the uranium concentration remained constant at 5.00 ± 0.14 mM up to 72 h. It was then rapidly removed from solution and was 0.24 ± 0.01 mM at 192 h, similar to the final concentration of uranium during photodegradation of the uranium–citrate complex.

Gas Production. Analysis of the headspace gas in the sealed samples showed the following amounts of carbon dioxide produced (μmol): iron–citrate, 480; uranium–citrate, 574; iron–uranium–citrate, 906. These amounts reflected the total concentration of citrate in the medium. A small amount of methane (0.12 μmol) was detected in the presence of uranium–citrate.

Characterization of Precipitates. *Metals Analyses.* Following photodegradation of the metal–citrate complexes, the solids were collected, dried, and weighed (Table 1). The precipitate from the photodegradation of the iron–citrate complex contained 52.5% iron by weight, the precipitate from photodegradation of the uranium–citrate complex contained 86.7% uranium by weight, and the precipitate from photodegradation of the iron–uranium–citrate complex contained 11.2% iron and 69.4% uranium by weight, respectively.

X-ray Diffraction. The X-ray diffraction results for the precipitates obtained from photodegradation of the metal–citrate complexes are presented in Figure 4. The ferrihydrite showed two broad peaks at approximately 34° and 62° 2θ, which is in the range of values for two-line ferrihydrite (*19*). The iron precipitate showed two broad peaks at approximately the same positions, which confirmed its identity

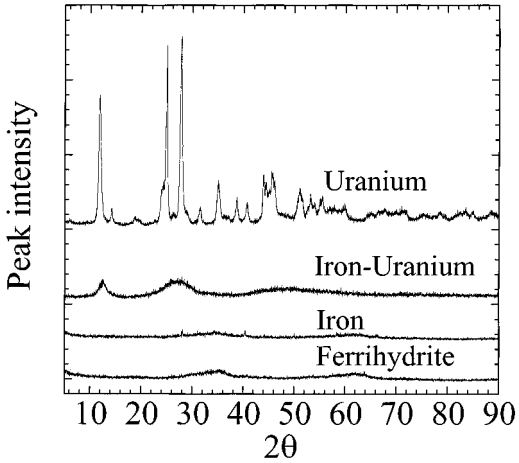

FIGURE 4. X-ray diffraction spectra for dried precipitates following photodegradation of iron−citrate, uranium−citrate, and iron−uranium−citrate complexes.

as two-line ferrihydrite. The 2θ values and peak intensities for the precipitated U are 27.6, 100; 24.8, 90; 11.8, 70; 43.7, 30; 45.8, 30; and 35.2, 20. The sharpness of the peaks indicate the crystalline nature of the material, and previous analysis has shown the precipitate to be similar to JCPDS 29-1376, identifying it as synthetic schoepite ($UO_3 \cdot 2H_2O$) (*6*). The Fe−U precipitate exhibited broad peaks at 12° and 27° 2θ, which are coincident with the major peaks in the schoepite sample. However, the amorphous nature of the sample and position of the major peaks suggests the presence of a uranyl hydroxide component (JCPDS 28-1415). There is a weak peak observed at 35° 2θ, which indicates the presence of ferrihydrite. The attenuation of the peak compared to this standard and iron−citrate sample indicates (i) the ferrihydrite is present as more amorphous form or (ii) uranium may play a role in inhibiting its formation.

EXAFS Analysis. The filtered k^3-weighted spectra (3.9−14.6 $Å^{-1}$) for the samples at the U L_{III} edge are presented in Figure 5A. The similarity in the EXAFS oscillations at low k indicate the equatorial oxygen atoms for the standard and precipitates are similar. This suggests a hydrated oxide or hydroxide structure for the samples. The complexity of the oscillations at higher k (>10 $Å^{-1}$), however, indicates the presence of a large backscatterer such as U.

Fourier transforms and fitting parameters for the precipitates are presented in Figure 5B and Table 2. The first shell coordination of 2.0−2.4 oxygens (O) at approximately 1.79−1.81 Å for all samples is due to the presence of double bonded axial (-yl) oxygens. The second and third shells are due to splitting of O atom distances in the U equatorial region. The uranyl hydroxide equatorial region contains 2.6 O's at 2.27 Å and 1.3 O's at 2.50 Å. The equatorial region for the U precipitate consists of 1.5 O's at 2.24 Å and 2.5 O's at 2.47 Å. In the mixed-metal precipitate, the near-neighbor equatorial atoms consist of 2.2 O's at 2.27 Å and 2.2 O's at 2.48 Å. The presence of a U−U interaction at 4.12 Å for uranyl hydroxide and at 4.06 Å for U precipitate is noted. In the precipitate resulting from photodegradation of the iron−uranium−citrate complex, the best fit consists of a U−U interaction at 4.13 Å. Attempts to fit the feature at approximately 2.9 Å with a uranium−iron interaction were unsuccessful. It has been noted that multiple scattering contributions from the *trans*-dioxo unit can give features in this region (*26*, *27*).

Discussion

The rate and extent of photodegradation of metal−citrate complexes and the degradation products varied with the type of metal. The structures for the iron−citrate, uranium−citrate, and iron−uranium−citrate complexes were determined using EXAFS, time-of-flight-secondary ion mass spectrometry (TOF-SIMS), gel filtration chromatography, and UV−vis spectrophotometry (*5*). The iron−citrate complex consisted of a binuclear iron unit coordinated to two citric acid molecules through carboxylate (μ-citrato) and oxy (μ-O) bridging groups (*5*). Titration data indicate all of the carboxylic acid groups are deprotonated. The mechanism of iron−citrate photodegradation is postulated to proceed according to the following reactions (1−3):

TABLE 2. EXAFS Structural Parameters for Precipitates Obtained from Photodegradation of Metal−Citrate Complexes[a]

sample	atom	*N*	*R*(Å)	σ^2	*F*
uranium−hydroxide	U−O_{ax}	2.0	1.81	0.0011	0.138
	U−O_{eq1}	2.6	2.27	0.0050	
	U−O_{eq2}	1.3	2.50	0.0032	
	U−U	1.0	4.12	0.0056	
uranium−precipitate	U−O_{ax}	2.4	1.79	0.0033	0.038
	U−O_{eq1}	1.5	2.24	0.0023	
	U−O_{eq2}	2.5	2.47	0.0044	
	U−U	1.0	4.06	0.0037	
uranium−iron precipitate	U−O_{ax}	2.2	1.80	0.0028	0.026
	U−O_{eq1}	2.2	2.27	0.0055	
	U−O_{eq2}	2.2	2.48	0.0032	
	U−U	1.0	4.13	0.0057	

[a] (*N*) coordination number, (*R*) interatomic distance, (σ^2) disorder parameter, and (*F*) overall goodness of fit parameter.

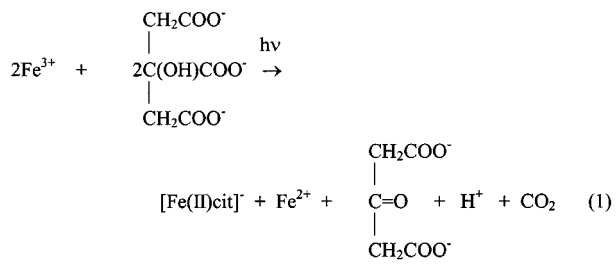

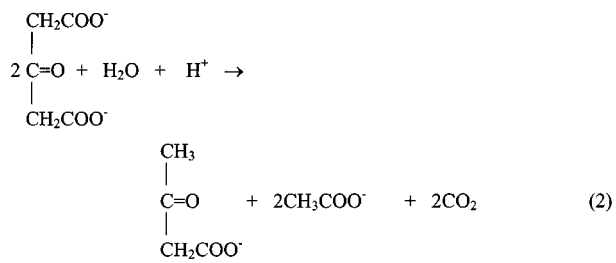

$$Fe^{2+}(Ligand) + O_2 + H_2O_2 \rightarrow Fe^{3+}(Ligand) + OH^- + {}^{\bullet}OH \rightarrow \text{ferrihydrite (ppt.)} + \text{products} \quad (3)$$

The primary photochemical mechanism is the intramolecular oxidation−reduction of the complex due to two one-electron ligand−metal charge transfers (LMCT) from one of the citric acid molecules to two ferric ions (reaction 1). The reaction results in formation of the iron(II)−citrate complex, ferrous ion, 3-oxoglutarate, hydrogen ion, and carbon dioxide. The 3-oxoglutarate undergoes autodecomposition to acetoacetate, acetate, and carbon dioxide (reaction 2). Production of 3-oxoglutarate and acetoacetate was observed when equimolar iron−citrate complex was exposed to sunlight under acidic conditions (*11*). The ferrous ion then undergoes oxidation to ferric ion, which precipitates from solution as ferrihydrite. Analysis of the mechanisms needed to account for the increased pH observed during photolysis suggests

that the photo-Fenton reaction is the primary source of hydroxyl ions. In this reaction, the ferrous ion undergoes oxidation to ferric ion in the presence of hydrogen peroxide and citric acid or reactive organic ligand intermediates (L) to generate 1 mol each of hydroxide ion and hydroxyl radical (reaction 3). Zepp et al. (*28*) and Kachur et al. (*29*) have shown that photolysis of the iron(III)−citrate complex results in the formation of ferrous ion and hydrogen peroxide, which then react to produce hydroxyl radicals. Regeneration of the ferrous ion occurs by oxidation of the citrate or organic ligand intermediate, as shown in reaction 1. Acetate, a product of the reaction, has been shown to undergo oxidation in the presence of amorphous ferrihydrite with significant generation of hydrogen peroxide (*30*).

The uranium−citrate is present in solution predominantly as a binuclear complex at pH 3.5. The uranium atoms are bridged by protonated hydroxyl groups (di-μ-OH), and complexation to citric acid occurs through the α-hydroxyl groups as well as the two terminal carboxylic acid groups (*5*, *7*). The photodegradation is proposed to proceed according to reactions 4−9:

$$[(UO_2)_2(Hcit)_2]^{2-} + 2H^+ \xrightarrow{h\nu} [HcitU(OH)_2)]^- + UO_2^{2+} + \begin{array}{c} CH_3 \\ | \\ C{=}O \\ | \\ CH_2COO^- \end{array} + CO_2 + H_2O \quad (4)$$

$$2\begin{array}{c} CH_3 \\ | \\ C{=}O \\ | \\ CH_2COO^- \end{array} + H_2O \rightarrow 2CH_3COO^- + \begin{array}{c} CH_3 \\ | \\ C{=}O \\ | \\ CH_3 \end{array} + CO_2 \quad (5)$$

$$[HcitU(OH)_2)]^- \xrightarrow{h\nu} [HcitUO(OH)]^- + H + O_2 \xrightarrow{\bullet O_2H} [HcitUO_2]^{2-} + H^+ \quad (6)$$

$$[HcitUO_2]^{2-} \rightarrow UO_2^+ + Hcit^{3-} \quad (7)$$

$$2UO_2^+ + 2H^+ \rightarrow UO_2^{2+} + UO^{2+} + H_2O \quad (8)$$

$$UO_2^{2+} + 3H_2O + \rightarrow UO_3 \bullet 2H_2O\ (ppt.) + 2H^+ \quad (9)$$

The photochemical reaction initially occurs via a two-electron-transfer mechanism, resulting in the formation of the uranium(IV)−citric acid complex $[HcitU(OH)_2)]^-$, acetoacetate, uranyl ion, carbon dioxide, and water (reaction 4). Acetoacetate is degraded by way of intramolecular rearrangement or a uranyl-sensitized photodecomposition reaction to acetate, acetone, and carbon dioxide (reaction 5). The tetravalent uranium is oxidized to uranyl ion by a complex set of photochemical reactions slightly modified from the original mechanism proposed by Adams and Smith (*31*). A photochemically generated hydrogen atom combines rapidly with dioxygen to produce the hydroperoxy radical $\bullet O_2H$. The uranium(IV)−citrate complex is then oxidized to a uranium(V)−citrate complex $[HcitUO_2]^{2-}$ (reaction 6). The weak pentavalent complex undergoes dissociation (reaction 7), followed by disproportionation to U(IV) and U(VI) ions (reaction 8). The U(VI) precipitates from solution as the mineral schoepite ($UO_3 \cdot 2H_2O$) (reaction 9), and the uranous

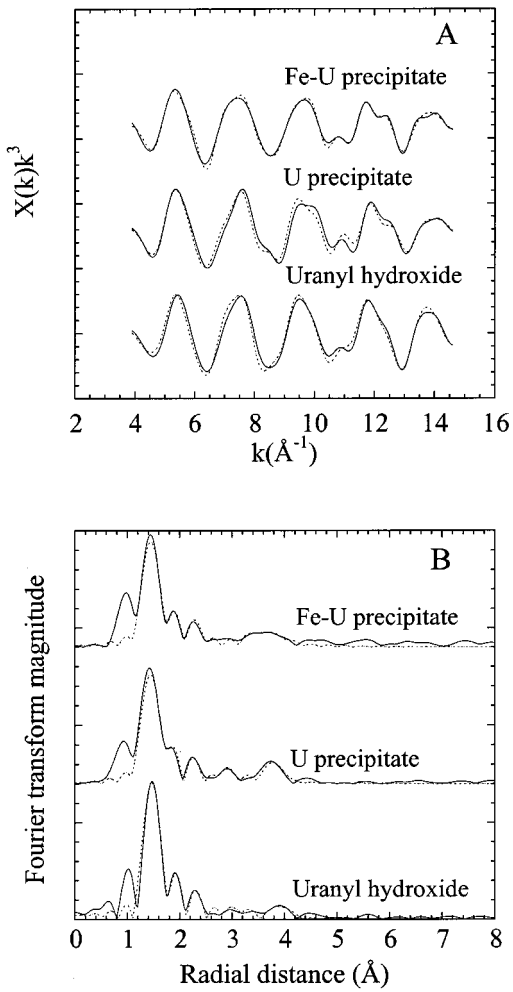

FIGURE 5. EXAFS spectra at the U L_{III} edge showing (A) Fourier-filtered k^3-weighted EXAFS spectra (3.9−14.6 Å^{-1}) and (B) Fourier transform for precipitates from photodegradation of uranium−citrate and iron−uranium−citrate complexes. Uranyl hydroxide is included as a reference standard.

ion may combine with citrate or organic intermediates to continue the photochemical reactions. The overall reaction involves a net consumption of hydrogen ions, which accounts for the increase in pH observed during the photodegradation.

The ternary iron−uranium−citrate complex structure consists of a binuclear iron core, similar to the iron−citrate complex, which is coordinated in bidentate fashion to two mononuclear tridentate uranium citrate complexes through the central carboxylate group of each citric acid (*5*). This unique configuration gives an overall stoichiometry for the complex of 2:2:4 iron−uranium−citric acid. The mechanism of photodegradation has not been previously proposed; therefore, we postulate that it occurs as follows (reactions 10 and 11):

$$[(UO_2cit)(Fe(III)cit)]_2^{2-} \xrightarrow{h\nu} [Fe(II)cit]^- + Fe^{2+} + 2[(UO_2)(cit)]^- + \begin{array}{c} CH_2COO^- \\ | \\ C{=}O \\ | \\ CH_2COO^- \end{array} + CO_2 + H^+ \quad (10)$$

$$Fe^{2+} + O_2 + H_2O_2 + [(UO_2)(cit)]^- \rightarrow [Fe(III)cit] + UO_2^{2+} + \bullet OH + OH^- \quad (11)$$

The initial reaction involves a two-step electron reduction of two ferric ions to ferrous ion and an iron(II)−citrate

complex, similar to the iron(III)−citrate reduction with concomitant oxidation of 1 mol of citric acid to 3-oxoglutarate, carbon dioxide, hydrogen ion, and the formation of a mononuclear uranium−citrate complex (reaction 10). The formation of a mononuclear complex from the photodegradation of a bridged binuclear cobalt(III)−pentaammine complex has been observed following reduction of Co(III) to Co(II) (*32*). Acetoacetate production results from autodecomposition (reaction 2). Acetone is produced as a result of uranyl-sensitized decomposition of 3-oxoglutarate (reaction 5). Ferric ion reduction is enhanced compared to that observed for the iron−citrate complex. However, uranyl ion does not undergo reduction. Redox inactivity of uranium may be due to the replacement of uranium in the mononuclear uranium−citrate complex, with ferric ion following the oxidation of ferrous ion by photo-Fenton reaction (reaction 11). It is noted that ferric ion remains in solution for up to 160 h before precipitation, while uranium slowly precipitates out at 96 h. This is much longer than observed for ferric ion in the presence of iron−citrate (96 h) and uranium as uranium citrate alone (3 h). The iron(III)−citrate complex, either as mononuclear or binuclear species, then undergoes photodegradation to organic acids with regeneration of ferric ion and the formation of ferrihydrite, as in reactions 1−3. The uncomplexed uranyl ion formed in reaction 11 precipitates from solution as a uranyl hydroxide species. The source of hydroxyl groups for uranium precipitation may be from the photo-Fenton reaction with iron or from hydrolytic reaction.

In summary, iron−citrate photodegradation occurred by two one-electron oxidations of citric acid to 3-oxoglutarate. Oxidation of ferrous ion by a photo-Fenton reaction resulted in its precipitation as two-line ferrihydrite. Uranium−citrate photodegradation occurred via a two electron-transfer process, resulting in the degradation of citric acid to acetoacetate and the reduction of uranyl ion to tetravalent form. Tetravalent uranium was photooxidized in the presence of dioxygen and precipitated as the mineral schoepite ($UO_3 \cdot 2H_2O$). The photodegradation of the iron−uranium−citrate complex resulted in its degradation to 3-oxoglutarate, a mononuclear uranium−citrate complex, and ferrous ion. Uranium did not undergo reduction; however, photooxidation of the iron to ferric form resulted in its precipitation as ferrihydrite. Uranium precipitated as a uranyl hydroxide species. The removal of other toxic metals and radionuclides from citric acid extracts of contaminated soils and wastes may be enhanced by the increase in pH observed during these studies.

Acknowledgments

We acknowledge the technical assistance of Kirk Mantione. This research was performed under the auspices of the Office of Science, Office of Biological and Environmental Research, and in part under Grant No. 64946, Environmental Management Science Program, Office of Science and Technology, Office of Environmental Management, U.S. Department of Energy (DOE) under Contract No. DE-AC02-98CH10886. However, any opinions, findings, conclusions, or recommendations expressed herein are those of the authors and do not necessarily reflect the views of DOE.

Literature Cited

(1) Francis, A. J.; Dodge C. J.; Gillow J. B. *Nature* **1992**, *356*, 140.
(2) Nunes, M. T.; Gill, V. M. S. *Inorg. Chim. Acta* **1987**, *129*, 283.
(3) Abrahamson, H. B.; Rezvani; A. B.; Brushmiller, J. G. *Inorg. Chim. Acta* **1994**, *226*, 117.
(4) Allen, P. G.; Shuh, D. K.; Bucher, J. J.; Edelstein, N. M.; Reich, T.; Denecke, M. A.; Nitsche, H. *Inorg. Chem.* **1996**, *35*, 784.
(5) Dodge, C. J. Ph.D. Dissertation, SUNY at Stony Brook, NY, 1999.
(6) Dodge, C. J.; Francis, A. J. *Environ. Sci. Technol.* **1994**, *28*, 1300.
(7) Rajan, K. S.; Martell, A. E. *Inorg. Chem.* **1965**, *4*, 462.
(8) Dodge, C. J.; Francis, A. J. *Environ. Sci. Technol.* **1997**, *31*, 3062.
(9) Manzurola, E.; Apelblat, A.; Markovits, G.; Levy, O. *J. Chem. Soc., Faraday Trans. 1* **1989**, *85* (2), 373.
(10) Sima, J.; Makanova, J. *Coord. Chem. Rev.* **1997**, *160*, 161.
(11) Frahn, J. L. *Aust. J. Chem.* **1958**, *11*, 399.
(12) Ohyoshi, A.; Ueno, K. *J. Inorg. Nucl. Chem.* **1974**, *36*, 379.
(13) Natarajan, P.; Endicott, J. F. *J. Phys. Chem.* **1973**, *77*, 1823.
(14) Hug, S. J.; Laubscher, H.-U.; James, B. R. *Environ. Sci. Technol.* **1997**, *31*, 160.
(15) Francis, A. J.; Dodge C. J. U.S. Patent No. 5,292,456, 1994.
(16) Francis, A. J.; Dodge, C. J. *Environ. Sci. Technol.* **1998**, *32*, 3993.
(17) Francis, A. J.; Dodge, C. J. *Appl. Environ. Microbiol.* **1993**, *59*, 109.
(18) Raven, K. P.; Jain, A.; Loeppert, R. H. *Environ. Sci. Technol.* **1998**, *32*, 344.
(19) Schwertmann, U.; Cornell, R. M. *Iron oxides in the laboratory*; VCH: Weinheim, Germany, 1991; p 91.
(20) *Standard methods for the examination of water and wastewater*, 14th ed.; American Public Health Association (APHA); Washington, D.C., 1975; p 208.
(21) Johnson, D. A.; Florence, T. M. *Anal. Chim. Acta* **1971**, *53*, 73.
(22) Cohen, D. *J. Inorg. Nucl. Chem.* **1970**, *32*, 3525.
(23) Rehr, J. J.; de Leon, M. M.; Zabinsky, S.; Albers, R. C. *J. Am. Chem. Soc.* **1991**, *113*, 5135.
(24) Ankudinov, A. Ph.D. Dissertation, University of Washington, WA, 1996.
(25) Heidt, L. J.; Moon, K. A. *J. Am. Chem. Soc.* **1953**, *75*, 5803.
(26) Hudson, E. A.; Allen, P. G.; Terminello, L. J. *Phys. Rev. B* **1996**, *54* (1), 156.
(27) Bargar. J. R.; Reitmeyer, R.; Lenhart, J. J.; Davis, J. A. *Geochim. Cosmochim. Acta* **2000**, *16*, 2737.
(28) Zepp, R. G.; Faust, B. C.; Holgne, J. *Environ. Sci. Technol.* **1992**, *26*, 313.
(29) Kachur, A. V.; Tuttle, S. W.; Biaglow, J. E. *Radiation Res.* **1998**, *150*, 475.
(30) Pekhonen, S. O.; Siefert, R.; Erel, Y.; Webb, S.; Hoffmann, M. R. *Environ. Sci. Technol.* **1993**, *27*, 2056.
(31) Adams, A.; Smith, T. D. *J. Chem. Soc.* **1960**, 4846.
(32) Balzani, V.; Carassiti, V. *Photochemistry of coordination compounds*; Academic Press: New York, 1970; p 226.

Received for review July 10, 2001. Revised manuscript received February 4, 2002. Accepted February 11, 2002.

ES011125M